

Estimation of Fracture path in the Structures and the Influences of Non-singular term on crack propagation

A.G. Khademalrasoul^{*1}
R. Maghsoudi²

Abstract

In the present research, a fully Automatic crack propagation as one of the most complicated issues in fracture mechanics is studied whether there is an inclusion or no inclusion in the structures. In this study The Extended Finite Element Method (XFEM) is utilized because of several drawbacks in standard finite element method in crack propagation modeling. Estimated Crack paths are obtained by using Level Set Method (LSM) in coupling with XFEM for 2D mixed mode crack propagation problems. Also, stress intensity factors for mixed mode crack problems are numerically calculated by using interaction integral method completely based on familiar path independent J-integral approach. However, the influence of the first non-singular term (T-stress) of Williams' stress distribution series in a cracked body is considered. Different crack growth paths are calculated for different domains with predefined notches such as edge and center cracks. In addition, predefined cracks and inclusions are implicitly defined using enrichment procedure in the XFEM framework and the effects of soft or hard inclusions are studied on crack propagation schemes. Finally, estimated crack paths under assumed conditions by using XFEM, are compared with the experimental results.

Keywords: Extended Finite Element Method, Level Set Method, Interaction integral, Soft and Hard inclusions, T-stress.

Received: 08 March 2017; Accepted: 20 June 2017

1. Introduction

Hydraulic structures are in a danger of cracking and the analysis of cracked hydraulic structure is very crucial for engineers. Dams and levees are some critical examples which propagating cracks can cause them to failure. Transverse and longitudinal cracking of embankment structures are common types of discontinuities in crown and the upstream/downstream slopes [1]. Also various types of cracks with random inclination angles in

¹ Faculty of Engineering, Department of Civil Engineering, Shahid Chamran University of Ahvaz, Ahvaz, Iran. (**Corresponding author**)

² Department of Civil Engineering, Esfarayen University of Technology, Esfarayen, North Khorasan, Iran.

concrete dams are possible. These strong discontinuities can arise from the date of construction or induced by fatigue phenomenon. When the structure has a strong discontinuity as long as subjected to loading, the crack will propagate. Therefore, large stress concentrations are avoided and a reasonable margin of security is taken to ensure that values close to the maximum admissible stress are never attained. Previous studies have demonstrated that structural failure might be happened in a lower applied loads; when there is a crack in the structure [11-13].

In such a case, the traditional finite element method cannot easily establish to simulate the propagating crack. Since in the finite element framework the domain of interest is defined by the mesh, therefore, the discontinuities have to be conformed onto the mesh [2, 3]. Consequently, at least for each increment of the crack growth, the domain surrounding the crack tip must be remeshed such that the updated crack geometry is accurately represented [4, 5]. However, In spite of progress of mesh generators, initial creation of the mesh with a crack and in the case of propagating crack, the modification of the initial mesh remains extremely heavy and difficult.

However, Extended finite element method (XFEM) is one of the capable numerical approaches in fracture mechanics [4, 18]. The combination of the XFEM by the Level Set Method (LSM) has been utilized to eliminate the cumbersome task of discontinuity modeling and the evolution of the internal discontinuous boundaries [19, 20]. The mathematical vision of the XFEM is based on the concept of discontinuous and asymptotic partition of unity enrichment (PUM) of the standard finite element approximation spaces. In the XFEM the discontinuities are conformed implicitly on the finite element domain [21]. In fact by using the additional degrees of freedom every kind of discontinuities are imposed on the solution field [22-25].

The first non-singular term of stress distribution series is called T -stress. The value of T -stress can be zero, positive or negative. T -stress significantly affects the shape and size of the plastic zone which develop at the vicinity of the crack tip. This term is a constant stress value and is independent of the distance to the crack tip. The T -stress is parallel to the crack surface. By considering the small-scale yielding condition, the effects of T -stress has been investigated on crack propagation problems [6-10].

Also, the concept of stress intensity factor (SIF) plays a central role in fracture mechanics. SIF depend on the geometry, crack length and loading conditions. Among several ways for evaluating the SIFs, the approaches which based on the concept of the energy are the most applicable methods [14-17]. According to the SIFs in mixed mode condition of loading, the crack propagation angle is calculated. Hence, the crack path would be predicted. The critical situation for an embankment is when the crack propagates and reaches to the dam's core. So, the estimation of the crack path is a crucial importance of dam safety monitoring.

Strong discontinuities (edge and center cracks), inclusions (soft or hard internal boundaries) and voids are created implicitly using enrichment procedure and any evolutions are taken into account by the level set definitions. In this research work the crack propagation in the presence of both soft and hard inclusions is studied in complicate conditions. To fulfillment of this objective a numerical computer program is prepared. In this computer code modeling of all types of internal heterogeneous boundaries are possible by using the level set approach. Therefore, without any internal excessive meshing or remeshing, internal boundaries are created in the finite element framework. Also, by using level set method any form of the conflict of internal boundaries are possible. Differences between maximum tangential stress (MTS) criterion and generalized MTS (GMTS) criterion are demonstrated.

The paper is outlined as follows; Section 2 presents the principle of linear elastic fracture mechanics and states the numerical calculation method of mixed-mode stress intensity factors. Section 3 is performed to introduce the principle of the enriched finite element method. Section

4 introduces the principles of the level set method. Numerical examples are listed in Section 5. Section 6 dedicates to conclude remarks.

2. Stress Intensity Factors

Behavior of a body with a discontinuity such as crack is generally characterized by a parameter such as stress intensity factors (SIFs) or path independent J -integral in linear elastic fracture mechanics. Also, during last decades much effort has been done on SIFs calculation. Theoretical, numerical and experimental methods have been employed for determination of the SIFs in the vicinity of the crack tips. According to two independent kinematic movements of upper and lower crack surfaces in 2D analysis, there are opening and sliding modes [15, 16, 26, 27]. Williams' asymptotic solution for crack-tip stress fields in any linear elastic body is given by a series of the form [28]:

$$\sigma_{ij}(r, \theta) = A_1 r^{-1/2} f_{ij}^{(1)}(\theta) + A_2 f_{ij}^{(2)}(\theta) + A_3 r^{1/2} f_{ij}^{(3)}(\theta) + \text{higher order terms}, \quad (1)$$

where σ_{ij} is the stress tensor, r and θ are polar coordinates with the origin at the crack tip (as shown in Figure 1). $f_{ij}^{(1)}, f_{ij}^{(2)}, f_{ij}^{(3)}$ are universal functions of θ , and A_1, A_2, A_3 are parameters proportional to remotely applied loads. In the vicinity of the crack tips, the leading term which exhibits a square-root singularity dominates. The amplitude of the singular stress fields is characterized by the SIFs, i.e. [28]

$$\sigma_{ij} = \frac{K_I}{\sqrt{2\pi r}} f_{ij}^I(\theta) + \frac{K_{II}}{\sqrt{2\pi r}} f_{ij}^{II}(\theta), \quad (2)$$

where K_I, K_{II} are the stress intensity factors for the opening (mode I) and shearing (mode II) modes respectively. However, the K field is not the exact solution to the stress field in a cracked body. It is the solution to the stress field as the crack tip is approached, where the approximations used in the derivation of the K field apply. The second term in the Williams' series solution (Eq. (1)) is a non-singular term, which is defined as the elastic T -stress. Thus the above expression (Eq. (2)) can be expanded to include this term as follows

$$\sigma_{ij} = \frac{K_I}{\sqrt{2\pi r}} f_{ij}^I(\theta) + \frac{K_{II}}{\sqrt{2\pi r}} f_{ij}^{II}(\theta) + T \delta_{ij} \delta_{1j}. \quad (3)$$

The T -stress varies with different crack geometries and loadings. It plays a dominant role on the shape and size of the plastic zone, the degree of local crack tip yielding, and also in quantifying fracture toughness. For mixed-mode problems, the T -stress contributes to the tangential stress and, as a result, it affects the crack growth criteria. By normalizing the T -stress with applied load $\sigma_0 (= K_I / \sqrt{\pi a})$, a is the crack length, a non-dimensional parameter B_T can be defined by [10, 29]

$$B_T = T \sqrt{\pi a} / K_I. \quad (4)$$

The dependence on geometrical configurations can be best indicated by the biaxiality parameter B_T .

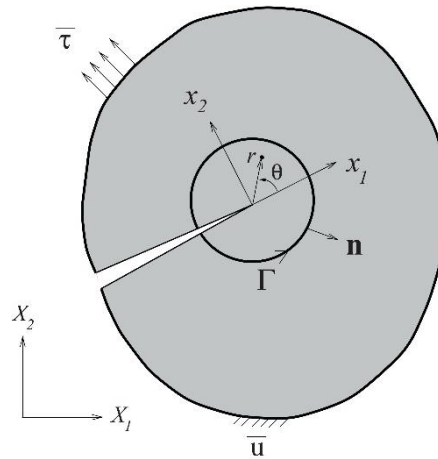


Figure 1. *Coordinate system and integration path, \bar{u} denotes prescribed displacement and $\bar{\tau}$ denotes prescribed tractions[30].*

2.1. M-integral

The *M*-integral is based on well-known path independent *J*-integral. The *J*-integral as a path independent integral, originally introduced by J.R. Rice to evaluate strain concentration by notches and cracks in a linear elastic or non-linear elastic and deformation-type elastic-plastic materials [31]. The *J*-integral is based on an energy balance and is equivalent to the energy release rate during crack extension in a homogeneous elastic body as follows[15]

$$\Pi_p(u_i) = \int_{\Omega} W(u_i) d\Omega - \int_{s_{\sigma}} \bar{T}_i u_i ds \tag{5}$$

$$J = - \frac{d \Pi_p}{da} \tag{6}$$

Consider a 2-D homogeneous crack body of linear or non-linear material free of body forces and tractions on the crack surfaces; the *J*-integral in numerical methods is usually defined as

$$J = \int_{\Gamma} \left[W(u_i) dx_2 - \sigma_{ij} n_j \frac{\partial u_i}{\partial x_1} ds \right], \tag{7}$$

where $W(u_i)$ is the strain energy density with the following preconditions

$$W(u_i) = W(x, y) = W(\epsilon) = \int_0^{\epsilon} \sigma_{ij} d\epsilon_{ij}$$

$$\sigma_{ij} = \frac{\partial W}{\partial \epsilon_{ij}} \quad (\text{Constitutive law}) \tag{8}$$

$$\epsilon_{ij} = \frac{1}{2}(u_{i,j} + u_{j,i}) \quad (\text{Compatibility})$$

$$\sigma_{ij,j} = 0 \quad \text{and} \quad \sigma_{ij} = \sigma_{ji} \quad (\text{Equilibrium})$$

A path-independent integral technique known as interaction integral method is used for evaluating mixed-mode stress intensity factors (SIFs). The *M*-integral is the dual form of the *J*-integral. The *M*-integral is based on the principle of complementary energy, while the *J*-integral is based on the principle of potential energy or strain energy density [15]. Also, due to simplification of the numerical calculations, the *M*-integral is formulated on an equivalent

domain area of integration as follows;

$$\begin{aligned} W(u_i) + B(\sigma_{ij}) &= \sigma_{ij} \varepsilon_{ij} \\ M &= \frac{d \Pi_c}{da} \\ \Pi_c(\sigma_{ij}) &= \int_{\Omega} B(\sigma_{ij}) d\Omega - \int_{S_u} \bar{u}_i \sigma_{ij} n_j ds \\ \varepsilon_{ij} &= \frac{\partial B}{\partial \sigma_{ij}} \end{aligned} \quad (9)$$

For general mixed mode problems in 2D analysis we have the following relationship between the values of J -integral and the stress intensity factors.

$$J = \frac{K_I^2 + K_{II}^2}{E_{eff}} \quad (10)$$

E_{eff} is defined in terms of material parameters E (Young's modulus) and ν (Poisson's ratio) as;

$$E_{eff} = \begin{cases} E, & \text{Plane Stress} \\ \frac{E}{1-\nu^2}, & \text{Plane Strain} \end{cases} \quad (11)$$

For defining the M -integral two states of a cracked body are considered. State 1 ($\sigma_{ij}^{(1)}, \varepsilon_{ij}^{(1)}, u_i^{(1)}$) corresponds to the actual state and state 2 ($\sigma_{ij}^{(2)}, \varepsilon_{ij}^{(2)}, u_i^{(2)}$) is an auxiliary state which will be chosen as the asymptotic fields for modes I and II. There are two sets of auxiliary fields for stress and displacements; (1) SIFs auxiliary fields and (2) auxiliary fields for the T -stress calculation [30, 32, 33]. The J integral for the sum of the two states is

$$J^{(1+2)} = \int_{\Gamma} \left[\frac{1}{2} (\sigma_{ij}^{(1)} + \sigma_{ij}^{(2)}) (\varepsilon_{ij}^{(1)} + \varepsilon_{ij}^{(2)}) \delta_{1j} - (\sigma_{ij}^{(1)} + \sigma_{ij}^{(2)}) \frac{\partial (u_i^1 + u_i^2)}{\partial x_1} \right] n_j d\Gamma \quad (12)$$

Expanding and rearranging terms gives

$$J^{(1+2)} = J^{(1)} + J^{(2)} + M^{(1,2)} \quad (13)$$

where $M^{(1,2)}$ is called the interaction integral for states 1 and 2

$$M^{(1,2)} = \int_{\Gamma} \left[W^{(1,2)} \delta_{1j} - \sigma_{ij}^{(1)} \frac{\partial u_i^2}{\partial x_1} - \sigma_{ij}^{(2)} \frac{\partial u_i^1}{\partial x_1} \right] n_j d\Gamma, \quad (14)$$

and $W^{(1,2)}$ is the interaction strain energy

$$W^{(1,2)} = \sigma_{ij}^{(1)} \varepsilon_{ij}^{(2)} = \sigma_{ij}^{(2)} \varepsilon_{ij}^{(1)} \quad (15)$$

Writing Eq (12) for 2D problems for the combined states gives after rearranging terms

$$J^{(1+2)} = J^{(1)} + J^{(2)} + \frac{2}{E_{eff}} (K_I^{(1)} K_I^{(2)} + K_{II}^{(1)} K_{II}^{(2)}) \quad (16)$$

Then from the Eq (16) and (13) we have the following relationship

$$M^{(1,2)} = \frac{2}{E_{eff}} (K_I^{(1)} K_I^{(2)} + K_{II}^{(1)} K_{II}^{(2)}) \quad (17)$$

Finally the stress intensity factors for the current state can be found by separating the two modes of fracture in 2-D problems. By selecting $K_I^{(2)} = 1$ and $K_{II}^{(2)} = 0$, we are able to solve for $K_I^{(1)}$ such that

$$K_I^{(1)} = \frac{I^{(1, Mode I)} E_{eff}}{2} \tag{18}$$

Then a similar procedure can be followed to calculate the $K_{II}^{(1)}$ from the interaction integral method for a mixed mode fracture problems. Also the contour integral defining $M^{(1,2)}$ is converted into an area integral by multiplying the integrand by a bounded smoothing function $q(\mathbf{x})$ that is 1 on an open set containing the crack tip and vanishes on an outer prescribed contour Γ_0 then for each contour Γ (as shown in Figure 2) in this open set where $q(\mathbf{x})=1$ and assuming the crack faces are stress free and straight in the interior of the region A bounded by the prescribed contour Γ_0 , the interaction integral may be written as

$$M^{(1,2)} = \int_C \left[W^{(1,2)} \delta_{1j} - \sigma_{ij}^{(1)} \frac{\partial u_i^2}{\partial x_1} - \sigma_{ij}^{(2)} \frac{\partial u_i^1}{\partial x_1} \right] q m_j d\Gamma, \tag{19}$$

where $C = \Gamma + C_+ + C_- + \Gamma_0$ and \mathbf{m} is the outward unit normal to the contour C . Now using divergence theorem and passing to the limit as the contour Γ is shrunk to the crack tip, which is justified by the dominated convergence theorem, gives the following equation for the interaction integral in domain form as[4]

$$M^{(1,2)} = \int_A \left[\sigma_{ij}^{(1)} \frac{\partial u_i^2}{\partial x_1} - \sigma_{ij}^{(2)} \frac{\partial u_i^1}{\partial x_1} - W^{(1,2)} \delta_{1j} \right] \frac{\partial q}{\partial x_j} dA \tag{20}$$

The condition that the smoothing function is 1 on an open set containing the crack tip is easily relaxed to be just equal 1 at the tip. The interaction integral is calculated using stresses and strains of the Gaussian integration points in the finite element framework.

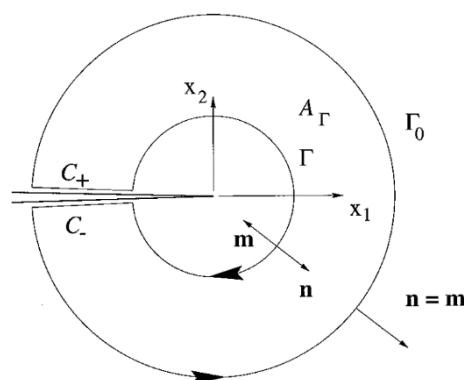


Figure 2. Equivalent domain for M-integral

2.2. Crack propagation angle

There are several approaches to predict the crack initiation angle for mixed mode fracture problems. The maximum tangential stress (MTS) criterion [34], the maximum energy release rate criterion[35], the minimum strain energy density criterion [36]. Based on the MTS criterion, a mixed mode crack propagates from the crack tip along the direction of maximum tangential stress, θ_c . According to this criterion, the direction of fracture initiation is determined from the following equation [37]:

$$\theta_c = 2 \arctan \frac{1}{4} \left(\frac{K_I}{K_{II}} - \text{sign}(K_{II}) \sqrt{\left(\frac{K_I}{K_{II}} \right)^2 + 8} \right), \quad (21)$$

where θ_c is given in the crack tip coordinate system, K_I and K_{II} are the mixed-mode stress intensity factors. The sign convention is such that $\theta_c < 0$ when $K_{II} > 0$ and vice versa.

In comparison with the conventional MTS criterion the generalized criterion makes use of a more accurate description for the crack tip stresses. It has been shown that [38] the tangential stress around the crack tip can be written as an infinite series expansion:

$$\sigma_{\theta\theta} = \frac{1}{\sqrt{2\pi r}} \cos \frac{\theta}{2} \left[K_I \cos^2 \frac{\theta}{2} - \frac{3}{2} K_{II} \sin \theta \right] + T \sin^2 \theta + O(r^{1/2}) \quad (21)$$

Where T -stress is the first non-singular term of series expansion. The higher order terms $O(r^{1/2})$ are assumed to be negligible near the crack tip. Unlike the MTS criterion in the generalized MTS (GMTS) the influences of the T -stress is considered on the fracture initiation direction. Therefore, according to the MTS criterion the direction of fracture initiation angle θ_c is determined from [29]:

$$\left. \frac{\partial \sigma_{\theta\theta}(r, \theta)}{\partial \theta} \right|_{\theta=\theta_c} = 0, \quad \frac{\partial^2 \sigma_{\theta\theta}(r, \theta)}{\partial \theta^2} < 0 \quad (22)$$

So

$$\left[K_I \sin \theta_c + K_{II} (3 \cos \theta_c - 1) \right] - \frac{16T}{3} \sqrt{2\pi r_c} \cos \theta_c \sin \frac{\theta_c}{2} = 0 \quad (23)$$

where r_c is the critical distance from the crack tip and is often considered as a constant material property. By normalizing T -stress and r_c as; $B = T \sqrt{\pi a / (K_I^2 + K_{II}^2)}$ and $\alpha = \sqrt{2r_c / a}$ the Eq. (23) can be written as follow

$$\left[K_I \sin \theta_c + K_{II} (3 \cos \theta_c - 1) \right] - \frac{16B \alpha \sqrt{K_I^2 + K_{II}^2}}{3} \cos \theta_c \sin \frac{\theta_c}{2} = 0 \quad (24)$$

2.3. T -stress calculation

Since T -stress is a constant stress that is parallel to the crack, the auxiliary stress and displacement fields are chosen to a point force f in the locally x_1 direction, applied to the tip of a semi-infinite crack in an infinite homogeneous plate, as shown in Figure 3. The auxiliary displacements are [39]

$$\begin{aligned} u_1^{aux} &= -\frac{f(1+\kappa)}{8\pi\mu} \ln \frac{r}{d} - \frac{f}{4\pi\mu} \sin^2 \theta \\ u_2^{aux} &= -\frac{f(\kappa-1)}{8\pi\mu} \theta + \frac{f}{4\pi\mu} \sin \theta \cos \theta \end{aligned} \quad (25)$$

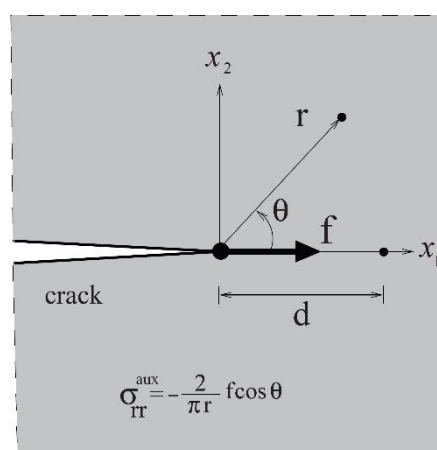


Figure 3. Local coordinates and point force f for T -stress calculation[30].

By considering the aforementioned auxiliary field, a simple expression for the T -stress in terms of the interaction integral (M -integral), the point force (f), and the material properties (E , ν) can be obtained.

$$T = \frac{E_{\text{eff}}}{f} M \quad (26)$$

where

$$f = - \lim_{\Gamma \rightarrow 0} \int_{\Gamma} \sigma_{ij}^{\text{aux}} n_j d\Gamma \quad (27)$$

3. Principles of Extended Finite Element Method

In the finite element method, the presence of flaws or inhomogeneities such as cracks, voids and inclusions must be taken into account in the mesh generation process. In the other hand the edges of the element must conform to these geometric entities. The XFEM aims to alleviate much of the burden associated with mesh generation for problems with any types of voids and interfaces by not requiring the finite element mesh to conform to the internal boundaries. The essence of the XFEM lies in sub-dividing a model into two parts: mesh generation for the domain which includes internal boundaries; and enriching the finite element approximation by additional functions that model the internal boundaries.

Extended finite element method has some special features in fracture mechanics. These special features of the extended finite element are due to partition of unity finite element (PUFEM) property of XFEM. The most prominent features of PUFEM are (1) the ability to include the local behavior of the solution in the finite element space, and (2) the ability to construct finite element spaces of any desired regularity. The XFEM can be assumed to be a classical FEM capable of handling arbitrary discontinuities. In fact, in The XFEM any types of discontinuities are modeled implicitly onto the domain of interest[40].The XFEM allows representing strong (cracks) and weak (holes, material interfaces) discontinuities. Arbitrarily oriented discontinuities can be modeled by enriching all elements cut by a discontinuity using standard enrichment functions. The enrichment functions should satisfy the discontinuous behavior and additional nodal degrees of freedom.

In the extended finite element method, first, the usual finite element mesh is produced, then, by considering the location of discontinuities, a few degrees of freedom are added to the classical finite element model in selected nodes near to the discontinuities .In the extended finite element method, the following approximation is utilized to calculate the displacement for the

point \mathbf{x} locating within the domain[41]

$$\mathbf{u}^h(\mathbf{x}_i) = \mathbf{u}^{\text{FE}} + \mathbf{u}^{\text{enr}} = \sum_{j=1}^n N_j(\mathbf{x}) \mathbf{u}_j + \left(\sum_{k=1}^m N_k(\mathbf{x}) v(\mathbf{x}) \mathbf{a}_k \right) \quad (28)$$

where n is the number of the nodes in the finite element mesh, $N_j(\mathbf{x})$ is the shape function of node j , \mathbf{u}_j are the classical degrees of freedom of node i and $v(\mathbf{x})$ is the enrichment function which is utilized to enrich the affected nodes by a discontinuity. Note that when there is no discontinuity in a domain the enrichment functions vanish. Since approximation in Eq. (28), does not satisfy the interpolation property; i.e., $\mathbf{u}_i \neq \mathbf{u}^h(\mathbf{x}_i)$ due to enriched degrees of freedom, the shifted enrichment function is employed to satisfy interpolation property[21].

3.1. Crack enrichment

In general, two different enrichment schemes are used for modeling a crack in homogeneous materials. Crack tip and Heaviside enrichment functions are implemented in the classical finite element method to the nodes of elements that influenced by the crack tip and body of the crack, respectively. It must be noted that there are different kinds of enrichment functions for strong and weak discontinuities in the XFEM. Figure 4, shows how classical FEM nodes are enriched to have an implicit crack on the domain of interest. For the elements which are completely cut by a crack body the Heaviside enrichment functions are employed as follows;

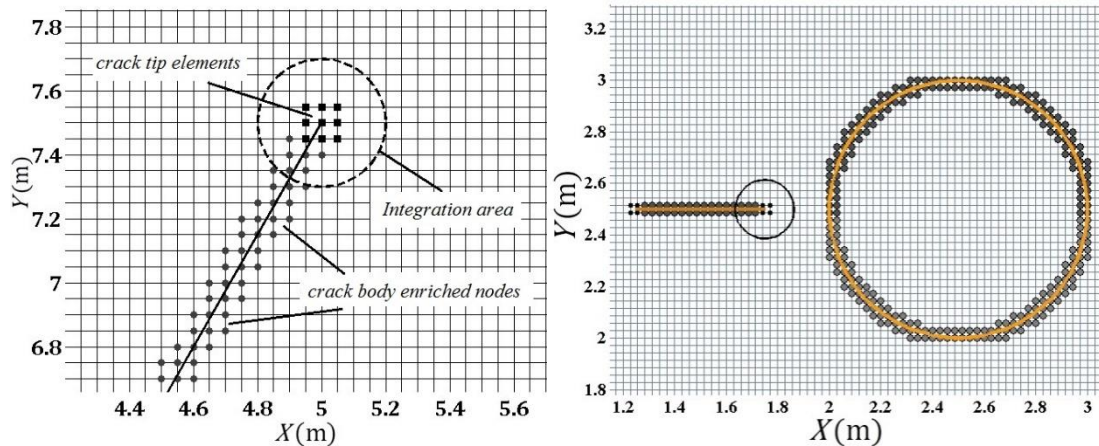


Figure 4. Crack tip and crack body enrichments with integration domain area (left), crack and inclusion enrichments (right).

$$H(x) = \begin{cases} +1 & \text{Above Crack} \\ -1 & \text{Below Crack} \end{cases} \quad (29)$$

For the case of an element containing the crack tip, the following four functions for the near tip displacement field are used. These asymptotic functions, originally introduced by Fleming for the representing crack tip displacement fields and repeated by Belytschko [18, 32, 42]. The crack tip enrichment functions are as follows

$$\{F_\alpha(x)\}_{\alpha=1-4} = \left\{ \sqrt{r} \sin \frac{\theta}{2}, \sqrt{r} \cos \frac{\theta}{2}, \sqrt{r} \sin \theta \cos \frac{\theta}{2}, \sqrt{r} \sin \theta \cos \frac{\theta}{2} \right\}, \quad (30)$$

where r and θ are the polar coordinates in the local crack tip coordinate system. When a

node would be enriched by both Eqs. (29) and (30) only Eq. (30) is used. In this research work the XFEM and Level Set Method (LSM) are coupled to model the discontinuities and subsequently find the trajectory of a crack due to different types of loading and boundary conditions.

3.2. Inclusion enrichment

Inclusions are inhomogeneities in a matrix with differing material properties. The modeling of inclusions requires the satisfaction of Hadamard condition, namely

$$\mathbf{F}^+ - \mathbf{F}^- = \mathbf{a} \otimes \mathbf{n}^+, \tag{31}$$

where \mathbf{F} is the deformation gradient, \mathbf{n}^+ is the outward normal to the material interface, and \mathbf{a} is an arbitrary vector in the plane. Sukumar was the first to try and represent a material interface using enrichment in XFEM[19]. This enrichment took the form as follow

$$\psi(x) = \left| \sum_I N_I(x) \zeta_I \right|, \tag{32}$$

where ζ_I are the nodal level set values for the material interface level set function. This solution however, leads to issues with blending between the enriched and unenriched elements. To improve the convergence rate a minimization problem was formulated which improved the convergence. Moes then addressed the problem using a modified absolute value enrichment where [43]

$$\psi(x) = \sum_I N_I(x) |\zeta_I| - \left| \sum_I N_I(x) \zeta_I \right|, \tag{33}$$

This enrichment was shown to have optimal convergence. In addition, note that the enrichment function goes to zero at all nodes such that it does not need to be shifted like many other enrichment functions.

4. Principles of Level Set Method

One of the major issues in problems with moving boundaries is how to track growth or moving of those boundaries [20, 44, 45]. Level set functions and fast marching methods are two capable approaches in tracking moving internal boundaries. Level set approach is based upon the idea of representing the interface as a level set curve of a higher-dimensional function $\phi(\mathbf{x}, t)$. A moving interface $\Gamma(t) \subset R^2$ can be formulated as the level set curve of a function $\phi: R^2 \times R \rightarrow R$, where

$$\Gamma(t) = \left\{ \mathbf{x} \in R^2 : \phi(\mathbf{x}, t) = 0 \right\}. \tag{34}$$

The Level Set Method (LSM) defines the surface of discontinuity by a signed distance function and models the evolution of the surface by a suitable evolution equation. The signed distance function is defined by a set of nodal values as Eq. (35), so no explicit representation of the crack is needed.

$$\phi(\mathbf{x}, t) = \pm \min_{\mathbf{x}_\Gamma \in \Gamma(t)} \|\mathbf{x} - \mathbf{x}_\Gamma\|, \tag{35}$$

where the sign is positive (negative) if \mathbf{x} is outside (inside) the contour defined by $\Gamma(t)$ (we assume that the interface $\Gamma(t)$ is such that one can define an interior and exterior to it). the evolution of the interface is then embedded in the evolution equation for ϕ , which is given by [44]

$$\begin{aligned} \varphi_t + F \|\nabla \varphi\| &= 0, \\ \varphi(\mathbf{x}, 0) & \text{ given,} \end{aligned} \quad (36)$$

where $F(\mathbf{x}, t)$ is the speed of the interface at $\Gamma(t)$ in the direction of the outward normal to the interface. The key advantages of this method are that it is computed on a fixed Eulerian mesh, handles topological changes in the interface naturally, and can easily be formulated in higher dimensions [20, 45, 46]. A schematic evolution of a given internal boundary is shown in Figure 5.

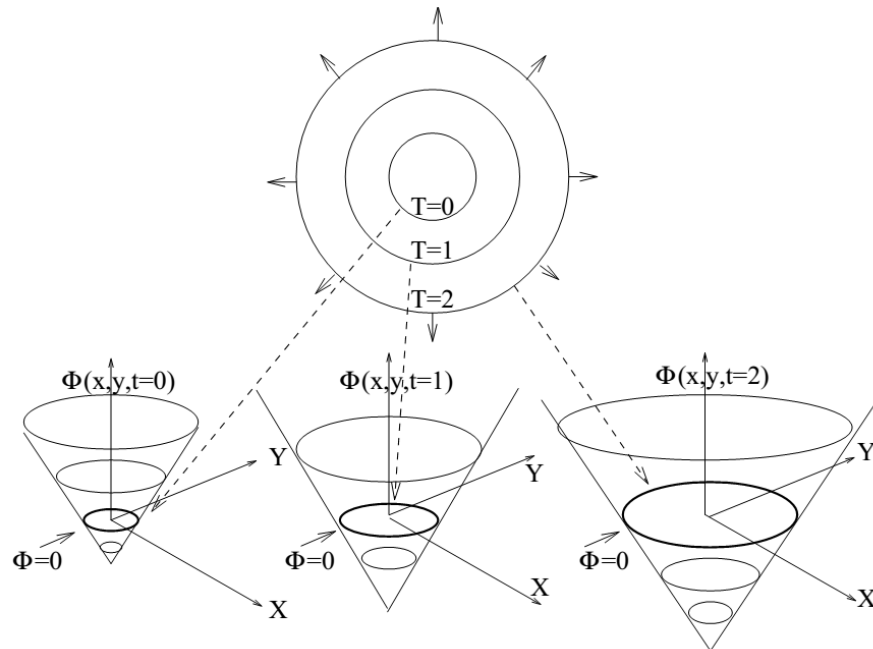


Figure 5. Transformation of front motion into initial value problem

In this study the initial crack geometry is represented by the Level Set functions in the XFEM framework, and subsequently signed distance functions are used to compute the enrichment functions that appear in the displacement-based finite element approximation. Rather than follow the interface itself, the Level Set approach instead takes the original interface and adds an extra dimension to the problem as shown in Figure 5. In fact, in the Level Set approach the height of the surface $\phi(x, y, t)$ which is defined as the z coordinate of the surface, is calculated to match the evolution of the interface in any time t . Thus to find out where the interface is at any time, cut the surface at zero height, in other words, plot the zero contour [19, 44, 47-49].

In this study by exploiting two level set functions $\phi(\mathbf{x}(t), t)$, $\psi(\mathbf{x}(t), t)$ in the XFEM framework for the crack tip and crack body respectively, the crack path is tracked. In this approach, the crack path is revealed by the zero level set of $\psi(\mathbf{x}(t), t)$. The zero level set function $\psi(\mathbf{x}(t), t)$ orientation passes from the crack tip position and oriented along the velocity function of the crack tip [50, 51].

Also it is noticeable that to speed up in the level set computations the “narrow band level set method” is used. For more information the reader can see [46]. Generally in this computational method, instead of performing calculations over the entire computational domain, an efficient modification is manipulated to perform work only in a neighborhood of the zero level set.

5. Numerical examples

In this section several models which contain crack (edge or center), inclusions and voids are studied. In the following examples different conditions of edge and center crack propagation will be evaluated. It should be noted that all examples are solved under the assumption of linear elastic behavior with small scale yielding condition. First of all, in order to establish the accuracy of calculations for stress intensity factors in mixed-mode of fracture, a comparison is done between numerical SIFs and theoretical values of counterpart.

Table 1 represents the accuracy of numerically calculated amounts of SIFs by using interaction integral in contrast with the theoretical values. It must be noted that the maximum error in obtained results according to Table 1 is 3%.

Table 1. Numerical and theoretical values of stress intensity factors in different conditions

Domain configuration	Crack length	Domain width	K_I Theoretical	K_I Numerical	K_{II} Theoretical	K_{II} Numerical
Center crack	1.0	6.0	1.2789	1.2536	0.0	-0.00008
Center crack	2.0	6.0	1.8915	1.8802	0.0	-0.0002
Center crack	0.25	20	0.7946	0.7698	0.0	-0.0002
Center crack	0.125	20	1.1263	1.1104	0.0	-0.0001
Center crack	0.1	20	1.2607	1.2475	0.0	-0.0001
Edge crack	0.5	3.0	1.6266	1.5986	0.0	-0.0005
Edge crack	1.0	3.0	3.1674	3.1687	0.0	0.0011

5.1. Domains with a Center-crack (CC)

In these examples a plate with a center crack are considered. In order to investigate the influences of loading conditions on the crack path, different types of loading are exerted on the boundary. Uniaxial tension, shear and mixed mode of loading are studied. In the first example a predefined horizontal center crack with the length of 0.5 in a 3×6 plate under uniaxial tension is modeled. In the second example a plate with a center crack under uniform shear is considered, and in the third example the mixed mode of loading is modeled. The constitutive material behavior is chosen as linear elastic with $E=210E^9$ (Pa) and $\nu = 0.3$. The models are discretized by using 91408 degrees of freedom. In addition to increase the integration accuracy around the crack tips a subtriangularization routine is used into the finite element code to refine the 4-nodequadrature's elements in the vicinity of the crack tips. The problems are solved under plane strain condition since SIFs are independent of the state of analysis.

In the first problem which is solved under given assumptions, the propagation of a horizontal center crack is simulated. As shown in Figure 6-left in the uniaxial tension the assumed crack, propagates horizontally due to the mode I predominance. However, according to the Figure 6-right which is considered under uniform shear (in positive direction) the crack path is completely different. This is arise from the facts of differences in the modes of fracture. In fact in the second example the mode II of fracture in predominance. And in the third example which is assumed under mixed-mode of loading (tension and shear) the center crack is propagating in a situation between two previous conditions. In fact the third example is the common type of hydraulic structures' failure. Because remote forces are applied on the structure due to the directional deformations (As shown in Figure 7).

It should be noted that in order to reduce the computational effort during the crack propagation only the affected part of the global stiffness matrix is updated. It is worthy to say that in all steps the candidates' elements and nodes to enriching have been chosen by the level

set functions.

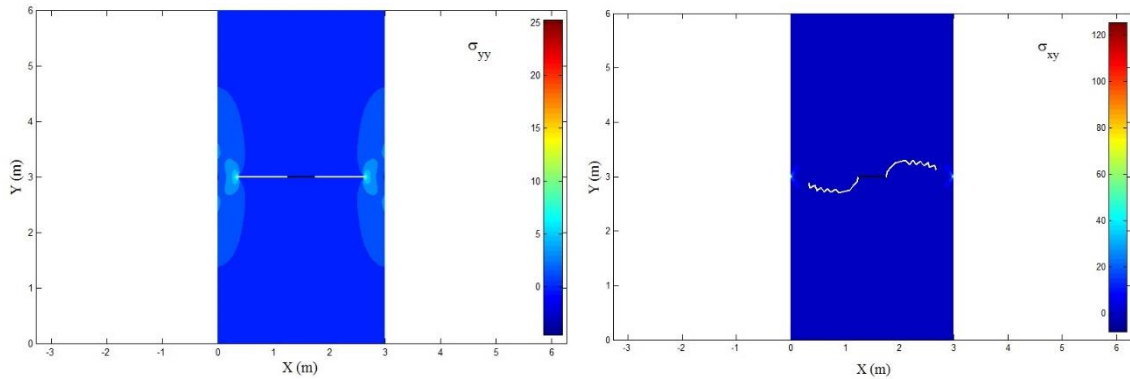


Figure 6. Center crack propagation: (left) under uniaxial tension, (right) uniform shear

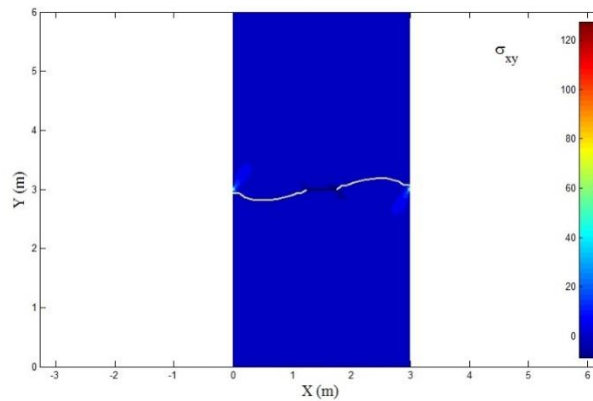


Figure 7. Mixed mode center crack propagation.

In the fourth and fifth examples of center crack propagation a 45 degrees oriented center crack under uniaxial tension and compression are modeled. Obviously these types of cracked domain is upon mixed-mode of fracture. In this problem the predicted crack growth paths are qualified by a laboratory Chalk specimen which was under simultaneous conditions. The results are shown in Figure 8. As depicted in Figure 8 both estimated and experimental crack growth paths are in the same situation. The main point in this problem is that both crack paths are going ahead perpendicular to the far faces. However, the numerical results are in the best accordance with the experimental result. In addition this minor mismatch could be due to the numerical errors. Different directions of crack propagations for an identical crack configuration in tension and compression is shown in Figure 9.

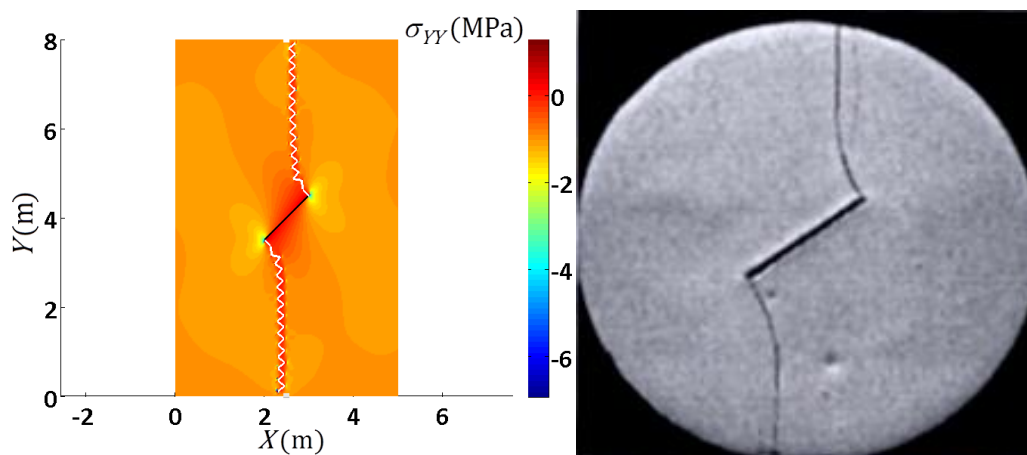


Figure 8. 45 degrees slanted center crack propagation. Numerical (left) and experimental results (right)

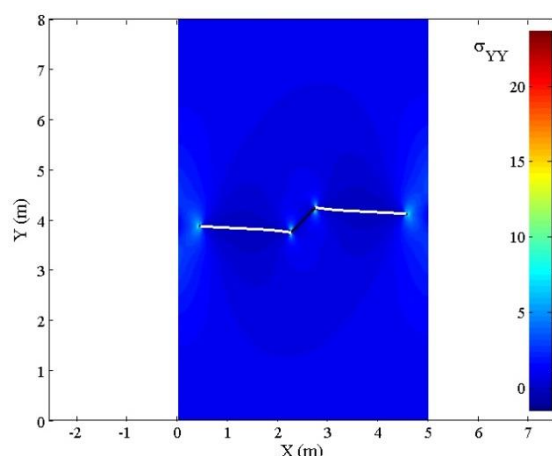


Figure 9. 45 degrees slanted center crack under tension.

Accordingly, crack propagation is dependent on the boundary conditions. As depicted in aforementioned examples, the loading condition mainly affects the stress intensity factors and finally the crack will propagate in opposite directions.

5.2. *T*-stress effects on crack propagation

In this section, the influences of considering the first non-singular term in the series expansion are studied. As if mentioned before this term participates in the shape and size of the plastic zone and finally affects the fracture initiation angle. In the following examples the crack initiation angles for the center crack with different orientations are shown. Based on the calculations for the horizontal and 45-degree center cracks in tension, no difference is achieved. In fact the crack paths for both are equal. The simulations are performed for tension and compression conditions. Figure 10 depicts the differences between fracture initiations for a 30-degree oriented center crack for tension and compression. In other words there is a significant difference in whether considering the *T*-stress effects in crack propagation or not.

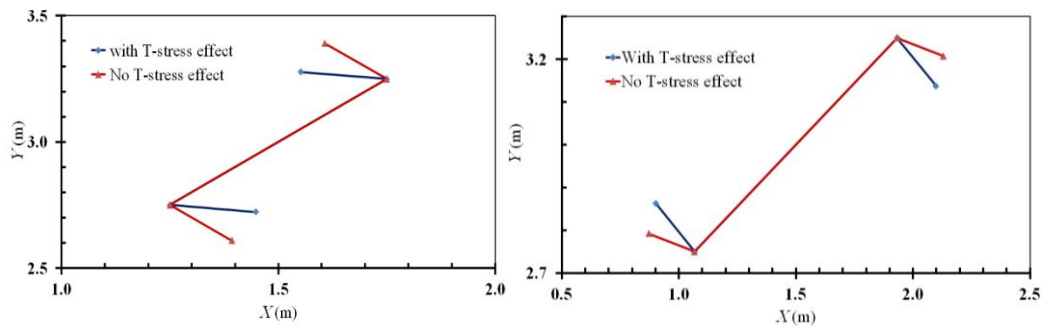


Figure 10. 30-degree slanted center crack: under compression (left), under tension (right)

Figure 11 illustrates a 45-degree slanted center crack propagations in tension and compression conditions. The T -stress effects are shown. As Figure 11 depicts, when the 45-degree oriented center crack is under tension, no different evidence between both conditions.

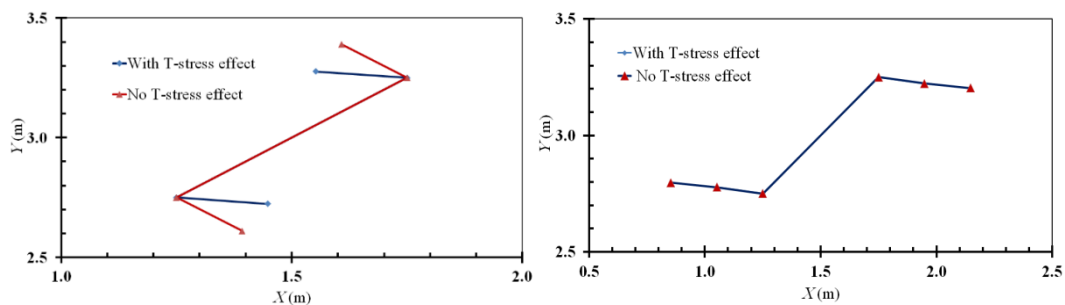


Figure 11. 45-degree slanted center crack: under compression (left), under tension (right)

Figure 12 illustrates a 60-degree slanted center crack propagations in tension and compression conditions. The T -stress effects are shown. As Figure 12 depicts, when the 60-degree oriented center crack is under tension, the aforementioned different decreases slightly. In fact, the crack configuration changes to a horizontal condition.

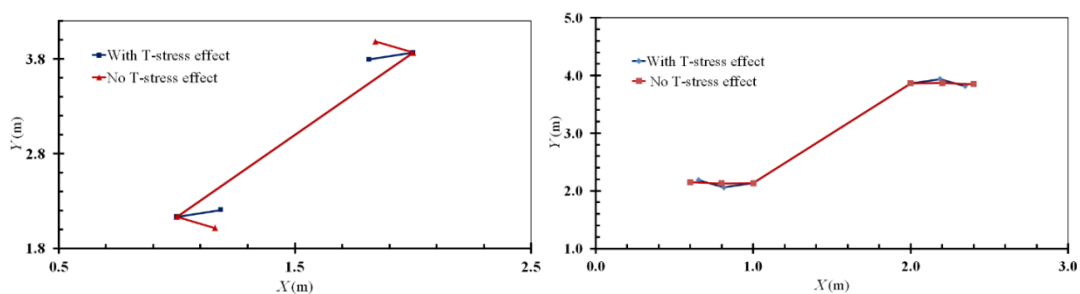


Figure 12. 60-degree slanted center crack: under compression (left), under tension (right)

5.3. Domains with an Edge-crack (EC)

In these examples a plate with an edge crack are considered. In order to investigate the influences of loading conditions on the crack path, different types of loading are exerted on the external boundary. Uniaxial tension, shear and mixed mode of loading are studied. In the first example a predefined horizontal centered edge crack with the length of 0.5 in a 3×6 plate under uniaxial tension is modeled. In the second example a plate with an off-centered edge crack under uniaxial tension is considered. The constitutive material behavior is chosen as linear elastic with

$E=210E^9$ (Pa) and $\nu = 0.3$. The models are discretized by using 91022 degrees of freedom. In fact a very fine quadratic mesh is used to accurately simulate the crack propagation. In addition to increase the integration accuracy around the crack tips a subtriangularization routine is used into the finite element code to refine the 4-node quadrature's elements in the vicinity of the crack tips. The problems are solved under plane strain condition since SIFs are independent of the state of analysis. Figure 13 illustrates the stress variations in a cracked body. In fact existence a discontinuity will change the stress distribution in the domain. In addition, the stress singularity because of the crack is well shown.

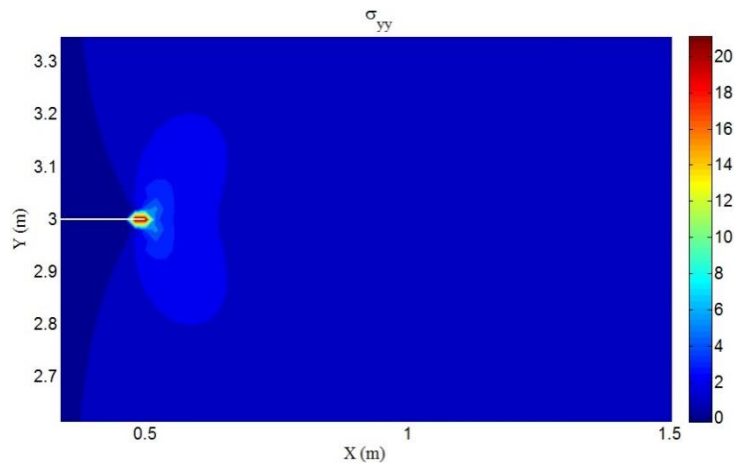


Figure 13. Stress distribution for a plate with a centered edge crack.

In the following examples the edge crack propagations under tension are simulated. First examples demonstrates the centered edge crack propagation under uniaxial tension, Figure 14-left depicts the crack path. Since uniaxial tension is applied, the crack extends horizontally in throughout the domain. However, in the second example in which an off-centered edge crack under uniaxial tension is considered. The crack propagates in a curvature path, that approaches the nearer geometrical boundary. Figure 14-right illustrates the curvature path for an off-centered edge crack.

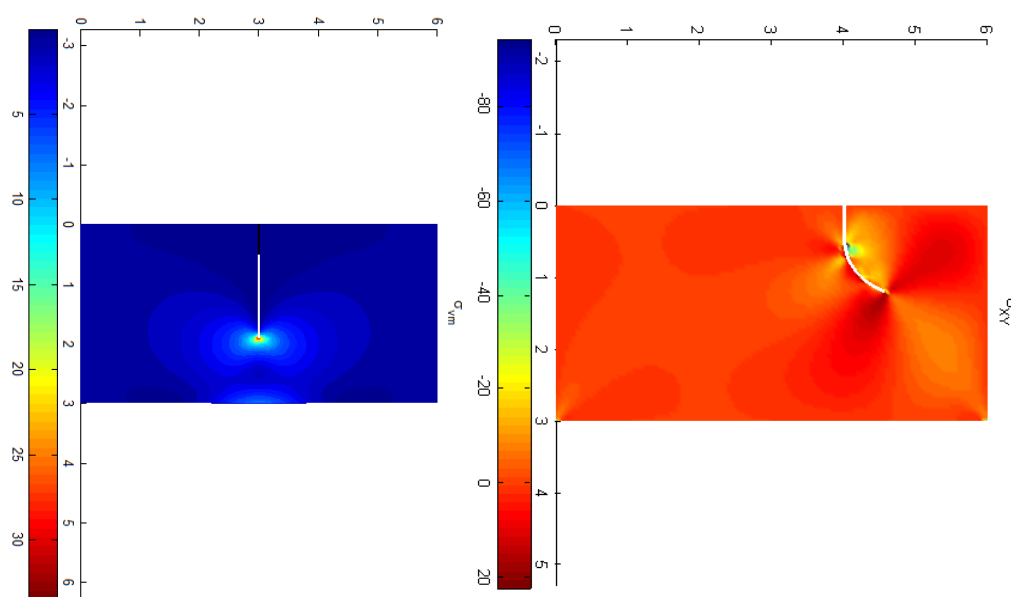


Figure 14. Edge crack propagation, centered edge crack (left), off-centered edge crack (right)

5.4. Edge-crack inclusion interaction

In this subsection the interaction between of an edge crack and both soft and hard inclusions are studied. One of the major aspects of the present study is the feasibility of modeling the different types of discontinuities simultaneously. Since presence of other discontinuities may affect the crack propagation path, therefore, the SIFs might varied due to the interactive behavior of the crack and inclusion. In fact in the crack-inclusion interaction problem there is an interface with a particular Young's modulus. When the Young's modulus of the interface is more than the Young's modulus of the material of the matrix, hard inclusion is exist and vice versa.

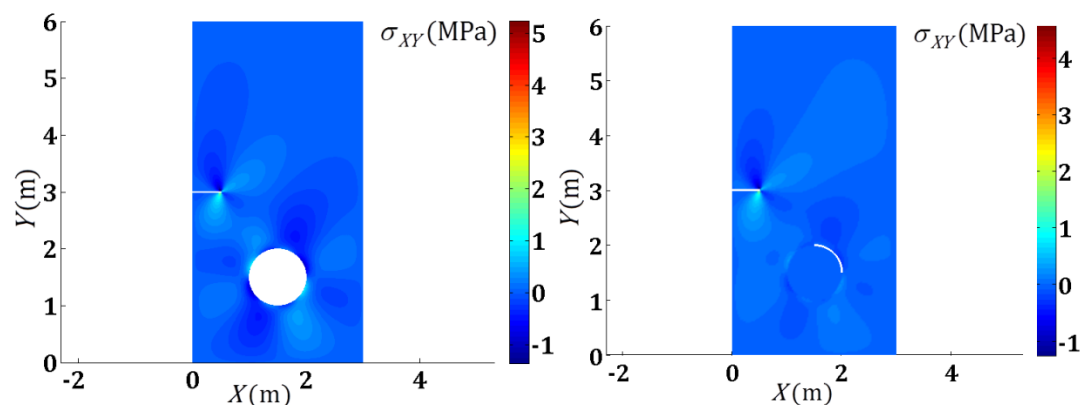


Figure 15 demonstrates the influences of the void\inclusion-crack interactions. As it shown and in the comparison with the Figure 13 the values of stresses due to the different discontinuities are affected. Table 2 shows the interactive stress intensity factors with different inclusions. In fact, the existence of the softer inclusions may change the SIFs to be greater than stiffer inclusions. Because the stresses magnify in the vicinity of the crack tips. Results are shown for a 0.5 edge crack length under uniaxial tension. Furthermore, the inclusion's diameter is chosen as 1.0. According to the numerical results, the horizontal edge crack propagation in the

interaction with the internal inclusions, is changed into the mixed-mode conditions. Since, crack-inclusion interaction mainly affects the mode II stress intensity factors. Therefore, the fracture initiations are not in the horizontal directions.

Table 2. The comparison between SIFs in the interaction with internal inclusions.

Domain configuration	Crack length	K_I	K_{II}
No inclusion	0.5	1.6239	-4.53E-8
Crack with soft inclusion	0.5	1.7483	0.0335
Crack with hard inclusion	0.5	1.5443	-0.0212
Crack with void	0.5	1.9839	0.1009

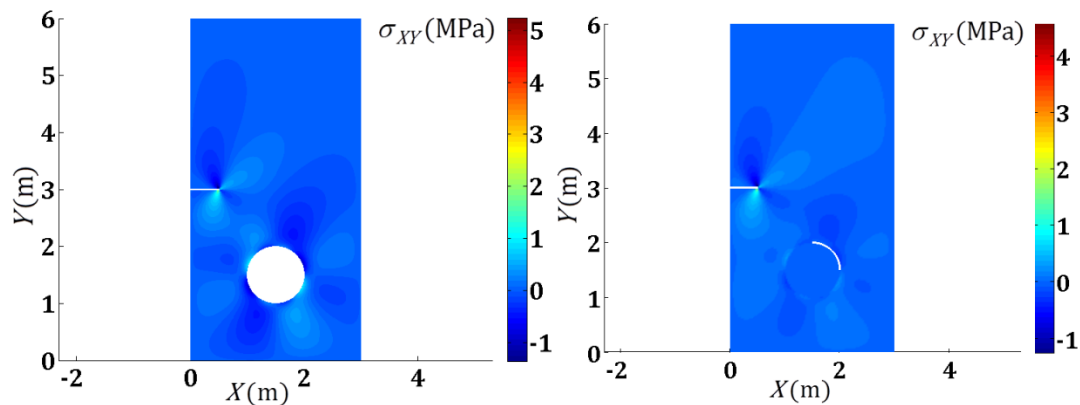


Figure 15. Crack-inclusion interaction problem: void-crack (left figure), and crack-inclusion (right figure)

One observes that, in the case of predefined cracked body with an interface as a hard inclusion the crack propagation path is moving away from the inclusion. This result may be very important in engineering design and crack propagation prediction in structural elements. In contrast, when there is a soft inclusion in the interaction with the crack, the soft inclusion attract the crack and the crack moves toward the soft inclusion.

6. Conclusion

The combination of the extended finite element method by the level set approach was performed to discontinuity modeling and evolutions of internal discontinuous boundaries. In the extended finite element framework all types of discontinuities were conformed implicitly on the finite element domain, therefore the interactions between different discontinuities were calculated. Edge and center cracks, inclusions (soft or hard internal boundaries) and voids were created implicitly and any evolutions were taken into account by the level set definitions. All procedures were numerically implemented in the finite element computer code to perform all calculations automatically. Subtriangularization was utilized to increase the accuracy of the numerical integration in the vicinity of the crack tips. The effects of soft or hard inclusions on the stress intensity factors and subsequently on the fracture initiation were demonstrated. Differences between maximum tangential stress (MTS) criterion and generalized MTS (GMTS) criterion were explained. In fact there were appreciable differences between crack initiations

with considering the effects of the first non-singular term of series expansion. It was shown that no different has occurred in the fracture initiation for a horizontal and 45-degrees slanted cracks under uniaxial tension. The computational values of the mixed-mode stress intensity factors are numerically calculated using dual form of J -integral and the values were in good accordance with the theoretical counterparts.

7. References

1. Sharma H D (1991) Embankment dams. New Delhi, Oxford & IBH Pub.
2. Giner E, Sukumar N, Tarancón J E, Fuenmayor F J. (2009). An Abaqus implementation of the extended finite element method. *Engineering Fracture Mechanics*, 76(3), 347-368.
3. Sukumar N, Prévost J H. (2003). Modeling quasi-static crack growth with the extended finite element method Part I: Computer implementation. *International Journal of Solids and Structures*, 40(26), 7513-7537.
4. Belytschko T, Black T. (1999). Elastic crack growth in finite elements with minimal remeshing. *International Journal for Numerical Methods in Engineering*, 45(5), 601-620.
5. Portela A, Aliabadi M H, Rooke D P. (1993). Dual boundary element incremental analysis of crack propagation. *Computers & Structures*, 46(2), 237-247.
6. Matvienko Y G, Pochinkov R A. (2013). Effect of nonsingular T-stress components on the plastic-deformation zones near the tip of a mode I crack. *Russian Metallurgy (Metally)*, 2013(4), 262-271.
7. Sobotka J C, Dodds Jr R H. (2011). T-stress effects on steady crack growth in a thin, ductile plate under small-scale yielding conditions: Three-dimensional modeling. *Engineering Fracture Mechanics*, 78(6), 1182-1200.
8. Sutradhar A, Paulino G H. (2004). Symmetric Galerkin boundary element computation of T-stress and stress intensity factors for mixed-mode cracks by the interaction integral method. *Engineering Analysis with Boundary Elements*, 28(11), 1335-1350.
9. Kim J-H, Paulino G H. (2003). T-stress, mixed-mode stress intensity factors, and crack initiation angles in functionally graded materials: a unified approach using the interaction integral method. *Computer Methods in Applied Mechanics and Engineering*, 192(11-12), 1463-1494.
10. Smith D J, Ayatollahi M R, Pavier M J. (2001). The role of T-stress in brittle fracture for linear elastic materials under mixed-mode loading. *Fatigue and Fracture of Engineering Materials and Structures*, 24(2), 137-150.
11. Zhuang Z, Liu Z, Cheng B, Liao J, (2014) Chapter 2 - Fundamental Linear Elastic Fracture Mechanics. In: Zhuang Z, Liu Z, Cheng B, Liao J, editors. *Extended Finite Element Method*. Oxford: Academic Press, pp. 13-31.
12. Zehnder A T (2012) *Fracture Mechanics*. Springer.
13. Gdoutos E E (2005) *Fracture Mechanics: An Introduction*. Springer.
14. Liang R Z, Rui Z C, Liang Z Y, Hong Z, *M-integral for Stress Intensity Factor Base on XFEM*, Third International Symposium on Electronic Commerce and Security Workshops, Guangzhou, China 226-230, 2010.
15. De Klerk A, Visser A G, Groenwold A A. (2008). Lower and upper bound estimation of isotropic and orthotropic fracture mechanics problems using elements with rotational degrees of freedom. *Communications in Numerical Methods in Engineering*, 24(5), 335-353.
16. Salvadori A, Gray L J. (2007). Analytical integrations and SIFs computation in 2D fracture mechanics. *International Journal for Numerical Methods in Engineering*, 70(4), 445-495.
17. Tur M, Giner E, Fuenmayor F J. (2006). A contour integral method to compute the generalized stress intensity factor in complete contacts under sliding conditions. *Tribology International*,

- 39(10), 1074-1083.
18. Fleming M, Chu Y A, Moran B, Belytschko T. (1997). Enriched element-free Galerkin Methods for Crack Tip Fields. *International Journal for Numerical Methods in Engineering*, 40(8), 1483-1504.
 19. Sukumar N, Chopp D L, Moës N, Belytschko T. (2001). Modeling holes and inclusions by level sets in the extended finite-element method. *Computer Methods in Applied Mechanics and Engineering*, 190(46-47), 6183-6200.
 20. Daru V. (2000). Level Set Methods and Fast Marching Methods – Evolving Interfaces in Computational Geometry, Fluid Mechanics, Computer Vision, and Materials Science by J.A. Sethian (Cambridge University Press, Cambridge, UK, 1999, 2nd edition, 378 pp.) £18.95 paperback ISBN 0 521 64557 3. *European Journal of Mechanics - B/Fluids*, 19(4), 531-532.
 21. Naderi R, Khademalrasoul A. (2015). Fully Automatic Crack Propagation Modeling in Interaction with Void and Inclusion without Remeshing *Modares Mechanical Engineering*, 15(7), 261-273.
 22. Bordas S, Nguyen P V, Dunant C, Guidoum A, Nguyen-Dang H. (2007). An extended finite element library. *International Journal for Numerical Methods in Engineering*, 71(6), 703-732.
 23. Sukumar N, Huang Z Y, Prévost J H, Suo Z. (2004). Partition of unity enrichment for bimaterial interface cracks. *International Journal for Numerical Methods in Engineering*, 59(8), 1075-1102.
 24. Moës N, Belytschko T. (2002). Extended finite element method for cohesive crack growth. *Engineering Fracture Mechanics*, 69(7), 813-833.
 25. Dolbow J, Moës N, Belytschko T. (2001). An extended finite element method for modeling crack growth with frictional contact. *Computer Methods in Applied Mechanics and Engineering*, 190(51-52), 6825-6846.
 26. Wu C-C, Xiao Q-Z, Yagawa G. (1998). Finite element methodology for path integrals in fracture mechanics. *International Journal for Numerical Methods in Engineering*, 43(1), 69-91.
 27. Yarema S Y. (1996). On the contribution of G. R. Irwin to fracture mechanics. *Materials Science*, 31(5), 617-623.
 28. Sutradhar A, Paulino G, Gray L J (2008) *Symmetric Galerkin Boundary Element Method*. Springer Berlin Heidelberg.
 29. Aliha M R M, Ayatollahi M R. (2012). Analysis of fracture initiation angle in some cracked ceramics using the generalized maximum tangential stress criterion. *International Journal of Solids and Structures*, 49(13), 1877-1883.
 30. Sutradhar A, Paulino G H, Gray L J (2008) *Symmetric Galerkin Boundary Element Method*. Springer-Verlag Berlin Heidelberg.
 31. Rice J R. (1968). A Path Independent Integral and the Approximate Analysis of Strain Concentration by Notches and Cracks. *Journal of Applied Mechanics*, 35(2), 379-386.
 32. Belytschko T, Fleming M. (1999). Smoothing, enrichment and contact in the element-free Galerkin method. *Computers and Structures*, 71(2), 173-195.
 33. Krongauz Y, Belytschko T. (1998). EFG approximation with discontinuous derivatives. *International Journal for Numerical Methods in Engineering*, 41(7), 1215-1233.
 34. Erdogan F, Sih G C. (1963). On the Crack Extension in Plates Under Plane Loading and Transverse Shear. *Journal of Basic Engineering*, 85(4), 519-525.
 35. Hussain M A, Pu S L, Underwood J. (1974). Strain energy release rate for a crack under combined mode I and Mode II. *Fracture Analysis*. ASTM STP 560).
 36. Sih G C, Kipp M E. (1974). Discussion on “fracture under complex stress—The angled crack problem”. *International Journal of Fracture*, 10(2), 261-265.
 37. Shih C F, Asaro R J. (1988). Elastic-Plastic Analysis of Cracks on Bimaterial Interfaces: Part

- I—Small Scale Yielding. *Journal of Applied Mechanics*, 55(2), 299-316.
38. Williams M L. (1957). On the stress distribution at the base of a stationary crack. *ASME Journal of Applied Mechanics*, 24(1), 109–114.
 39. Timoshenko S, Goodier J N (1982) *Theory of elasticity*. 3rd edn. Auckland, McGraw-Hill.
 40. Melenk J M, Babuška I. (1996). The partition of unity finite element method: Basic theory and applications. *Computer Methods in Applied Mechanics and Engineering*, 139(1–4), 289-314.
 41. Giner E, Sukumar N, Denia F D, Fuenmayor F J. (2008). Extended finite element method for fretting fatigue crack propagation. *International Journal of Solids and Structures*, 45(22–23), 5675-5687.
 42. Belytschko T, Krongauz Y, Organ D, Fleming M, Krysl P. (1996). Meshless methods: An overview and recent developments. *Computer Methods in Applied Mechanics and Engineering*, 139(1–4), 3-47.
 43. Moës N, Cloirec M, Cartraud P, Remacle J F. (2003). A computational approach to handle complex microstructure geometries. *Computer Methods in Applied Mechanics and Engineering*, 192(28–30), 3163-3177.
 44. Osher S, Sethian J A. (1988). Fronts propagating with curvature-dependent speed: algorithms based on Hamilton-Jacobi formulations. *Journal of Computational Physics*, 79(1), 12-49.
 45. Sethian J A. (1996). A fast marching level set method for monotonically advancing fronts. *Proceedings of the National Academy of Sciences*, 93(4), 1591-1595.
 46. Adalsteinsson D, Sethian J A. (1995). A Fast Level Set Method for Propagating Interfaces. *Journal of Computational Physics*, 118(2), 269-277.
 47. Shi J, Chopp D, Lua J, Sukumar N, Belytschko T. (2010). Abaqus implementation of extended finite element method using a level set representation for three-dimensional fatigue crack growth and life predictions. *Engineering Fracture Mechanics*, 77(14), 2840-2863.
 48. Sukumar N, Chopp D L, Moran B. (2003). Extended finite element method and fast marching method for three-dimensional fatigue crack propagation. *Engineering Fracture Mechanics*, 70(1), 29-48.
 49. Chopp D L, Sukumar N. (2003). Fatigue crack propagation of multiple coplanar cracks with the coupled extended finite element/fast marching method. *International Journal of Engineering Science*, 41(8), 845-869.
 50. Stolarska M, Chopp D L. (2003). Modeling thermal fatigue cracking in integrated circuits by level sets and the extended finite element method. *International Journal of Engineering Science*, 41(20), 2381-2410.
 51. Stolarska M, Chopp D L, Moës N, Belytschko T. (2001). Modelling crack growth by level sets in the extended finite element method. *International Journal for Numerical Methods in Engineering*, 51(8), 943-960.